38

Electromagnetic Fields Generated by Earthquakes

M.J.S. Johnston
US Geological Survey, Menlo Park, USA

1. Introduction

Independent knowledge of the physical processes that occur with seismic events can be obtained from observations of electric and magnetic fields generated by these complex processes. During the past few decades, we have seen a remarkable increase in the quality and quantity of electromagnetic (EM) data recorded before and during earthquakes and volcanic eruptions. This paper describes the most significant recent data and the implications these data have for different generating mechanisms. We note that, despite several decades of relatively high quality monitoring, clear demonstration of the existence of precursory EM signals has not been achieved, although causal relations between coseismic magnetic field changes and earthquake stress drops are no longer in question. This paper extends discussions of tectonomagnetism and tectonoelectricity, over the various parts of the electromagnetic spectrum from radio frequencies (RF) to submicrohertz frequencies, that are covered in Johnston (1989, 1997), Park *et al*. (1993), Park (1996) special journal issues (Johnston and Parrot, 1989, 1998; Parrot and Johnston, 1993), and books (Hayakawa and Fujinawa, 1994).

2. History

Suggestions that electromagnetic field disturbances are a consequence of the earthquake failure process have been made throughout recorded history. Some of the earliest work (Milne, 1890, 1894) refers to magnetic fields observed during the Great Lisbon earthquake in 1799. However, these early observations, and others during the nineteenth century (Mascart, 1887; Milne, 1894), were recognized as spurious by Reid (1914) who showed that traces recorded by magnetographs located close to earthquake epicenters were produced by inertial effects, not magnetic disturbances. This invalidated all earlier reports based on records of magnetic variometers, which are simply suspended magnets. Later data up through the mid-20th century recorded on fluxgate magnetometers are similarly suspect because these instruments are sensitive to displacements and rotations common in the epicentral regions during the propagation of seismic waves. It was not until the mid-1960s that meaningful results were obtained following the advent of absolute magnetometers, use of noise reduction techniques, and hardening of magnetometer measurement systems against the effects of earthquake accelerations and displacements. This is apparent in a plot of signal amplitude as a function of time, shown in Figure 1. Post-1960s data are generally considered trustworthy provided care has been taken to ensure sensors are insensitive to seismic shaking and are in regions of low-magnetic-field gradient.

Together with better stability against shaking, an impressive improvement in sensors, sensor reliability, data collection

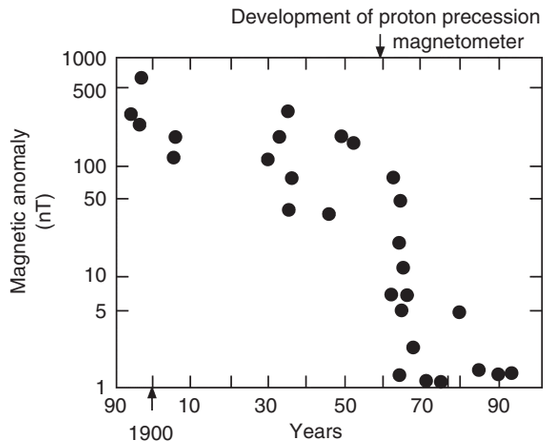

FIGURE 1 Reported amplitudes of tectonomagnetic anomalies as a function of time. "P" indicates the time at which absolute proton precession magnetometers and noise reduction techniques were introduced (updated from Rikitake, 1968).

Au. Q: Pl. chk **"P"** does not appear in the figure

INTERNATIONAL HANDBOOK OF EARTHQUAKE AND ENGINEERING SEISMOLOGY, VOLUME 81A

techniques, analysis, and international cooperation has also been apparent during the past few years. Largely as a consequence, reliable observations of magnetic, electric and electromagnetic field variations, related to seismic events and tectonic stress/strain loading, have been obtained on faults in Japan, China, Russia, California, and several other locations.

3. Statement of the Problem

This chapter reviews recent results of magnetic, electric, and electromagnetic disturbances apparently associated with earthquakes and discusses the physical mechanisms likely to have produced them. Although some observations are larger than expected, the best field observations are generally in agreement with calculations. Some observations are suggested as precursors yet have no corresponding co-event signals and some have co-event signals yet no precursory signals. More field observations are clearly needed and more careful work needs to be done to demonstrate convincingly causality, or lack thereof, between EM signals and earthquakes. In particular, further improvement is needed with the use of multiple detectors, use of multiple reference sites, application of noise identification/reduction procedures. Most important is the demonstration of consistency and correlation with other geophysical data that independently reflect the state of stress, strain, material properties, fluid content, and approach to failure of the Earth's crust in seismically active regions.

4. Summary of Physical Mechanisms Involved

The loading and rupture of water-saturated crustal rocks during earthquakes, together with fluid/gas movement, stress redistribution, and change in material properties, has long been expected to generate associated magnetic and electric field perturbations. The detection of related perturbations prior to fault rupture has thus been proposed frequently as a simple and inexpensive method to monitor the state of crustal stress and perhaps to provide tools for predicting crustal failure (Wilson, 1922; Kalashnikov, 1954; Stacey, 1964; Stacey *et al*., 1965; Yamazaki, 1965; Brace and Orange, 1968a,b; Nagata, 1969; Barsukov, 1972; Rikitake, 1968, 1976; Honkura *et al*., 1976; Fitterman, 1979, 1981; Ishido and Mizutani, 1981; Varotsos and Alexopoulos, 1987; Dobrovolsky *et al*., 1989; Sasai, 1980, 1991a,b; Park, 1991; Fujinawa *et al*., 1992; Fenoglio *et al*., 1995; Utada, 1993). The primary mechanisms for generation of electric and magnetic fields with crustal deformation and earthquake-related fault failure include piezomagnetism, stress/conductivity, electrokinetic effects, charge generation processes, charge dispersion, magnetohydrodynamic effects, and thermal remagnetization and demagnetization effects. Discussion of the different mechanisms will be roughly in order of the degree of attention that has been accorded them.

4.1 Piezomagnetism

The magnetic properties of rocks have been shown under laboratory conditions to depend on the state of applied stress (Wilson, 1922; Kalashnikov and Kapitsa, 1952; Kapitsa, 1955; Ohnaka and Kinoshita, 1968; Kean *et al*., 1976; Revol *et al*., 1977; Martin, 1980; Pike *et al*., 1981). Theoretical models have been developed in terms of single domain and pseudo-single domain rotation (Stacey, 1962; Nagata, 1969; Stacey and Johnston, 1972) and multidomain wall translation (Kern, 1961; Kean *et al*., 1976; Revol *et al*., 1977). The fractional change in magnetization per unit volume as a function of stress, can be expressed in the form;

$$\Delta I \approx K\sigma \cdot I \tag{1}$$

where ΔI is the change in magnetization in a body with net magnetization I due to a deviatoric stress σ. K, the stress sensitivity, typically has values of about $3 \times 10^{-3}\,\mathrm{MPa}^{-1}$. The stress sensitivity of induced and remanent magnetization from theoretical and experimental studies has been combined with stress estimates from dislocation models of fault rupture and elastic pressure loading in active volcanoes to calculate magnetic field changes expected to accompany earthquakes and volcanoes (Stacey, 1964; Stacey *et al*., 1965; Shamsi and Stacey, 1969; Johnston, 1978; Davis *et al*., 1979; Sasai, 1980, 1983, 1991a,b; Davis *et al*., 1984; Johnston *et al*., 1994; Banks *et al*., 1991). The surface fields (ΔB_P) at a point, P, can be calculated in two ways: (1) by either integrating the change in magnetization ΔI_Q in a unit volume, dv, at a point Q where the stress is σ_{ij}, and r is the distance between P and Q, according to,

$$\Delta B_P = -\frac{\mu}{4\pi}\nabla \int_V \Delta I_Q \cdot \frac{r}{r^3}\, dv \tag{2}$$

as originally done by Stacey (1964), or (2) by using a simpler method pioneered by Sasai (1980, 1994) in which analytic expressions of the surface piezomagnetic potential, W, produced by a known stress distribution in a magnetoelastic half-space are obtained by transforming the stress matrix and integrating over the magnetized region. In this latter case, the surface field can be found from:

$$\Delta B_P = -\nabla W \tag{3}$$

These models show that magnetic anomalies of a few nanoteslas (nT) should be expected to accompany earthquakes for rock magnetizations and stress sensitivities of 1 ampere/meter ($\mathrm{A\,m}^{-1}$) and $10^{-3}\,\mathrm{MPa}^{-1}$, respectively. As shown below, these signals are readily observed with the correct sign and amplitude.

4.2 Stress/Resistivity and Strain/Resistivity effects

In a like manner, the stress dependence of electrical resistivity of rocks has been demonstrated in the laboratory. Resistivity in low porosity crystalline rock increases with compression as a result of crack closure at about 0.2%/bar (Brace *et al*., 1965) and decreases with shear due to crack opening at about 0.1%/bar (Yamazaki, 1965; Brace and Orange, 1968a,b; Brace, 1975). More porous rocks have even lower stress sensitivity. The situation is further complicated by the fact that nonlinear strain can also produce resistivity changes (Lockner and Byerlee, 1986). A stress/resistivity relation equivalent to Eq. (1) has the scalar form

$$\frac{\Delta\rho}{\rho} \approx K_r \sigma \tag{4}$$

for homogeneous material, where ρ is resistivity, K_r is a constant, and σ is the stress. Unfortunately, the earth is not homogeneous and many factors including rock type, crack distribution, degree of saturation, porosity, strain level, etc., can localize or attenuate current flow. Nevertheless, this equation provides a starting point for calculating resistivity changes near active faults. Measurements of resistivity change are being made with both active experiments (where low frequency currents are injected into the ground and potential differences, V, are measured on receiver dipoles), or passive telluric and magnetotelluric (MT) experiments where changes in resistivity are inferred from changes in telluric or MT transfer functions. These transfer functions are given by:

$$Z(\omega) = \frac{E(\omega)}{H(\omega)} \tag{5}$$

where ω is angular frequency, $E(\omega)$ and $H(\omega)$ are observed electric and magnetic fields. For active experiments (Park *et al*., 1993),

$$\frac{\delta\rho}{\rho} = G\frac{\delta V}{V} \tag{6}$$

where δV is the change in potential difference and G is a constant. For MT experiments,

$$\delta\rho = \frac{\delta|Z(\omega)|^2}{\omega\mu} \tag{7}$$

Based on the field observations of stress changes accompanying earthquakes (≈ 1 MPa), resistivity changes of at least 1% might be expected to accompany crustal failure. Field experiments for detection of resistivity changes thus need to have a measurement precision of better than 0.1% (Fitterman and Madden, 1977; Park, 1991; Park *et al*., 1993). This may be difficult with MT measurements unless remote magnetic field reference measurements are used (Gamble *et al*., 1979) although measurement precision for telluric electric fields can be made at the 0.1% level (Madden *et al*., 1993).

4.3 Electrokinetic Effects

The role of active fluid flow in the Earth's crust as a result of fault failure can generate electric and magnetic fields (Mizutani and Ishido, 1976; Fitterman, 1978, 1979; Ishido and Mizutani, 1981; Dobrovolsky *et al*., 1989; Fenoglio *et al*., 1995). Electrokinetic electric and magnetic fields result from fluid flow through the crust in the presence of an electric double layer at the solid–liquid interfaces. This double layer consists of ions anchored to the solid phase, with equivalent ionic charge of opposite sign distributed in the liquid phase near the interface. Fluid flow in this system transports the ions in the fluid in the direction of flow, and electric currents result. Conservation of mass arguments (Fenoglio *et al*., 1995) supported by surface strain observations (Johnston *et al*., 1987) limit this process in extent and time because large-scale fluid flow cannot continue for very long before generating easily detectable surface deformation.

The current density j and fluid flow v are found from coupled equations (Nourbehecht, 1963; Fitterman, 1979) given by

$$j = -s\nabla E - \frac{\xi\zeta\nabla P}{\eta} \tag{8}$$

$$v = \frac{\phi\xi\zeta\nabla E}{\eta} - \frac{\kappa\nabla P}{\eta} \tag{9}$$

where E is streaming potential, s is the electrical conductivity of the fluid, ξ is the dielectric constant of water, η is fluid viscosity, ζ is the zeta potential, ϕ is the porosity, κ is the permeability, and P is pore pressure.

The current density in Eq. (8) has two components. The second term represents electric current resulting from mechanical energy being applied to the system and is sometimes called the "impressed" current (Williamson and Kaufman, 1981). This term describes current generated by fluid flow in fractures. The first term of Eq. (8) represents "back" currents resulting from the electric field generated by fluid flow. The distribution of electrical conductivity determines the net far-field magnetic and electric fields resulting from these effects. In an extreme case, if the fluid is extremely conducting and the surrounding region is not, current flow in the fluid cancels the potential generated by fluid flow (Ahmad, 1964). At the other extreme, if the fluid is poorly conducting, "back" currents, usually termed "volume currents" (Williamson and Kaufman, 1981) flow in the surrounding region. If the region were homogeneous, magnetic fields would be generated by impressed currents only since the volume currents generate no net field (Fitterman, 1979; Fenoglio *et al*., 1995). The situation for finite flow in limited fault fractures more closely

approximates the second case where the surface magnetic field is approximately given by:

$$B = \frac{\mu_0}{4\pi} \int_A \frac{j_i \times r}{r^2}\, dA \tag{10}$$

where μ_0 is the magnetic permeability in free space. Note that, the physics describing the electric and magnetic fields generated in the human body as blood is pumped through in arteries provides a very good analog to those generated in fault zones (Williamson and Kaufman, 1981). This occurs because the electrical conductivities of bone ($0.001\,\mathrm{S\,m^{-1}}$), muscle ($0.1\,\mathrm{S\,m^{-1}}$) and blood ($1\,\mathrm{S\,m^{-1}}$) and blood velocities are similar to those of rock, fault gouge, fault zone fluids, and the likely fluid velocities determined by Darcy Law fluid diffusion in fault zones. Considerable work has been done in understanding the physics of electric and magnetic field generation in the human body and this can be applied directly to crustal faulting situations. Reasonable fault models, in which fluid flows into a 200 m long rupturing fracture at a depth of 17 km, indicate that transient surface electric fields of several tens of millivolts per kilometer and transient magnetic fields of a few nT can be generated (Fenoglio *et al*., 1995).

4.4 Charge Generation Processes

Numerous charge generation mechanisms have been suggested as potential current sources for electric and magnetic fields before and during earthquakes. These mechanisms include piezoelectric effects (Finkelstein *et al*., 1973; Baird and Kennan, 1985), triboelectricity effects produced by rock shearing (Lowell and Rose-Innes, 1980; Gokhberg *et al*., 1982; Brady, 1992), fluid disruption/vaporization (Blanchard, 1964; Matteson, 1971; Chalmers, 1976), and solid state mechanisms (Dologlou-Revelioti and Varotsos, 1986; Freund *et al*., 1992). Each of these mechanisms has a solid physical basis supported by laboratory experiments on either dry rocks in insulating environments or single crystals of dry quartz. Each is capable of producing substantial charge under the right conditions. However, at least two fundamental problems need to be studied in the application of charge-generation processes to EM field generation in the Earth's crust. The first concerns the amplitude of each charge generation effect in wet rocks at temperatures and pressures expected in the Earth's crust and the second concerns charge maintenance time and propagation in the conducting crust.

Regarding the first problem, experiments clearly need to be done for each mechanism to quantify the effects expected in wet rocks at temperatures of at least 100°C and at confining pressures of 100 MPa expected at earthquake hypocenters. Experiments on dry rocks at atmospheric pressure are not very relevant to this issue. Piezoelectric effects in dry quartz bearing rocks are less than 0.1% of those observed for single crystals of quartz due to self canceling effects (Tuck *et al*., 1977; Sasaoka *et al*., 1998), and effects in wet rocks will likely be smaller still and transient at best. EM generation by fracturing dry rocks (Warwick *et al*., 1982; Brady, 1992) needs to be extended to wet rocks under confining pressure. Experiments on hole transport of O_- in dry rocks (Freund *et al*., 1992) and stress charging of dry nonpiezoelectric rocks (Dologlou-Revelioti and Varotsos, 1986) need also to be repeated with wet rocks under confining pressure so that these effects can be quantified. Brady (1992) observed no EM emission during fracture of conductive rocks since the conductor could not maintain charge separation.

The second fundamental problem concerns the discharge time for these processes and just how far EM signals generated by them might propagate. The charge relaxation time τ for electrostatic processes is given by the product of permittivity (ε) and resistivity (ρ). ε is $0.5\text{–}1.0 \times 10^{-10}\,\mathrm{F\,m^{-1}}$ for crustal rocks. If $\rho \approx 10^3$ ohm.m (typical upper value for near fault crustal rock) then,

$$\tau \approx 10^{-6}\,\mathrm{sec} \tag{11}$$

Although polarization effects (Lockner and Byerlee, 1985) will generate somewhat longer timescales (perhaps as much as a second), EM signal generation by charge generation processes must necessarily still be very rapid unless mechanisms can be found for isolating and maintaining large charge densities in a conducting earth. Furthermore, dispersion precludes EM fields propagating very far in a conducting earth (Honkura and Kuwata, 1993).

Attenuation of the magnetic field, B, of a plane electromagnetic wave generated at depth by charge generation/cancellation processes as a function of penetration distance through a conductive medium is given by:

$$B = B_0 e^{-\gamma z} \tag{12}$$

where B_0 is the initial field strength, z is the penetration distance into the medium, and γ is the complex propagation coefficient given by:

$$\gamma = \sqrt{\omega^2 \mu\varepsilon + j\omega\mu s} \tag{13}$$

where ω is the angular frequency of the radiation, μ is the magnetic permeability of the earth, ε is the permittivity, and s is the conductivity of the medium. If s is $0.1\,\mathrm{S\,m^{-1}}$, the frequency is 0.01 Hz, the "skin depth" is 10 km, so fields generated at this depth could be observable at the earth's surface.

If these fields are generated by rock cracking and fracturing, acoustic (seismic) signals should also be generated (see Lockner *et al*., 1991). Seismic wave attenuation with distance z has the form

$$A(z) = A_0 \exp^{-(\omega z/2cQ)} \tag{14}$$

where ω is the angular frequency, c is the phase velocity, and Q is the quality factor. Taking observed values of 3 km sec^{-1} and 30 for c and Q, it can easily be shown that seismic waves in the frequency band 1–0.01 Hz are not attenuated significantly in the epicentral area. At higher frequencies, both seismic and EM signals are heavily attenuated. For example, at 10 Hz the EM "skin depth" is 493 m in material with conductivity of 0.1 S m^{-1} and the seismic equivalent "penetration depth" is 2864 m. At 100 Hz the comparative depths are 156 m, 286 m, and at 1 KHz 29 m, 49 m, respectively.

Thus, both high frequency seismic and EM waves are heavily attenuated in the earth's crust. EM sources at 10 Hz should have an acoustic component that is more easily detected over a greater area. In fact, for all EM sources at seismogenic depths capable of propagating to the earth's surface (i.e., with frequencies less than 0.1 Hz), acoustic/seismic consequences of these sources propagate more effectively to the surface and might be used to verify their existence.

4.5 Magnetohydrodynamic (MHD) Effects

The induced magnetic field B_i generated by the motion v of a fluid with conductivity s in a magnetic field B_0, is governed by the equation:

$$\frac{\partial B}{\partial t} = \nabla \times v \times B + \frac{\nabla^2 B}{\mu_0 s} + \frac{\nabla s \times \nabla \times B}{\mu_0 s^2} \qquad (15)$$

where μ_0 is the permeability in a vacuum (Shercliff, 1965). For low magnetic fields and low electrical conductivities in the Earth's crust where the fluid motion is not affected by the induced fields, the induced field is given approximately by the product of the magnetic Reynolds number R_m and the imposed field B_0, i.e.,

$$B_i \approx R_m \times B_0 \approx \mu s v \, d B_0 \qquad (16)$$

where d is the length scale of the flow. Critical parameters here are the likely flow velocities and fluid electrical conductivities in the crust. Flow velocity is determined by rock permeability and fluid pressure gradients according to Darcy's Law. Permeability of fractured rock is not less than 10^{-12} m^2 (Brace, 1980) and pore-pressure gradients cannot exceed the lithospheric gradient. It is difficult to achieve widespread flow velocities of even a few millimeters sec^{-1} with this mechanism. Furthermore, fluid conductivities are unlikely to exceed that of sea water ($\approx$ 1 S m^{-1}). Using these numbers, fluid flow in fractured fault zones at seismogenic depths ($\approx$ 5 km) with a length scale of 1 km could generate transient fields of about 0.01 nT. This is far too small to be observed at the Earth's surface. As a check on these calculations, we note that fields of a few nT are observed with waves in the ocean where the conductivity is 1 S m^{-1} and wave velocities exceed 100 cm sec^{-1} (Fraser, 1966).

4.6 Thermal Remagnetization and Demagnetization

Crustal rocks lose their magnetization when temperatures exceed the Curie Point ($\approx$ 580°C for magnetite) and become remagnetized again as the temperature drops below this value. Stacey and Banerjee (1974) describe this process in detail. In crustal rocks at seismogenic depths near active faults, this process is unlikely to contribute to rapid changes in local magnetic fields since the thermal diffusivity of rock is typically about 10^{-6} m^2 sec^{-1} and migration of the Curie Point isotherm by conduction cannot be as much as a meter in a year (Stacey, 1992). At shallow depths in volcanic regions, particularly in recently emplaced extrusions and intrusions, thermal cracking with gas and fluid movement can transport heat rapidly and large local anomalies can be quickly generated (Rikitake and Yokoyama, 1955; Hurst and Christoffel, 1973; Emeleus, 1977; Zlotnicki and Le Mouel, 1988; Hamano *et al*., 1990; Dzurisin *et al*., 1990; Zlotnicki and Le Mouel, 1990; Tanaka, 1993, 1995). These anomalies can be modeled as a magnetized slab in a half-space. Good examples of magnetic modeling of anomalies generated by cooling of extrusions can be found in Dzurisin *et al*. (1990) for Mt. St. Helens and in Tanaka (1995) for Mt. Unzen in Japan. Some seasonal variations may result from annual temperature diffusion into magnetic rocks in the upper few meters of the Earth's crust (Utada *et al*., 2000).

5. Experimental Design and Measurement Precision

5.1 Basic Measurement Limitations

The precision of local magnetic and electric field measurements on active faults varies as a function of frequency, spatial scale, instrument type, and site location. Most measurement systems on the Earth's surface are limited more by noise generated by ionosphere, magnetosphere, and by cultural noise than by instrumental noise. Thus, systems for quantifying these noise sources are of crucial importance if changes in electromagnetic fields are to be uniquely identified. For spatial scales of a few kilometers to an few tens of kilometers, comparable to moderate magnitude earthquake sources, geomagnetic and electric noise power decreases with frequency as $1/f^2$, similar to the "red" spectrum behavior of most geophysical parameters (Johnston *et al*., 1984). Figure 2 shows an example of a noise power spectrum for two typical sites 10 km apart on the San Andreas fault in regions of low local magnetic gradient and far from sources of cultural noise (after Ware *et al*., 1985).

Against this background noise, transient magnetic fields can be measured to several nanotesla over months, to 1 nT over days, to 0.1 nT over minutes, and 0.01 nT over seconds. Long-term changes and field offsets can be determined if their amplitudes exceed about 1 nT. Comparable electric field noise

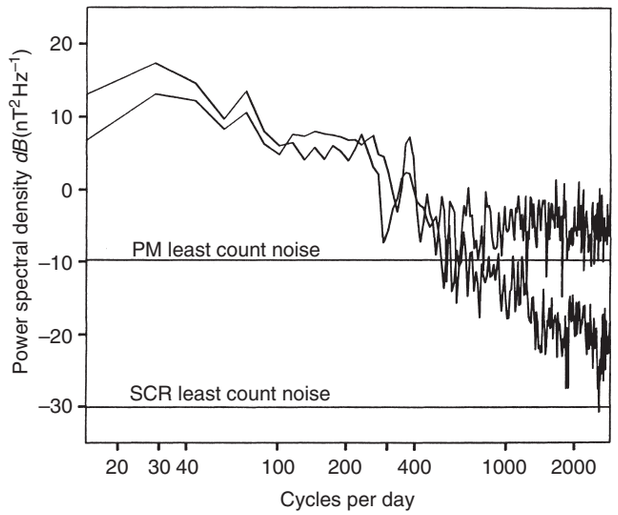

FIGURE 2 Power spectral density of simultaneous differences between sites 10 km apart on the San Andreas fault near San Juan Bautista. The self-calibrating rubidium (SCR) data are consecutive 10 sec measurements with a 0.014 nT least count. The 0.125 least-count proton magnetometer (PM) data are 1.5 sec averages taken every 15 sec (after Ware *et al*., 1985).

limits are 10 mv km^{-1} over months, several mv km^{-1} over days, 1 mv km^{-1} over minutes and 0.1 mv km^{-1} over seconds (derived from Park, 1991). EM noise increases approximately linearly with site separation (Johnston *et al*., 1984). Cultural noise further complicates measurement capability because of its inherent unpredictability. This largely precludes measurements in urban areas.

5.2 Experimental Techniques

Thus, unambiguous observations of EM signals originating within the Earth's crust require well-planned experiments to discriminate against these ionospheric, magnetospheric, and cultural noise sources. At lower frequencies (microhertz to hertz) for both electric and magnetic field measurements, the most common technique involves the use of reference sites with synchronized data sampling in arrays using site spacing comparable to the expected source sizes of a few kilometers (Rikitake, 1966; Johnston *et al*., 1984; Park and Fitterman, 1990; Park 1991; Varotsos and Lazaridou, 1991). This relatively simple system allows as much as a 30 dB reduction in noise (Park, 1991; Johnston *et al*., 1984). Techniques for further noise reduction such as adaptive filtering (Davis *et al*., 1981; Davis and Johnston, 1983), use of multiple variable-length sensors in the same and nearby locations (Varotsos and Alexopoulos, 1987; Mori *et al*., 1993), provide about a factor of three further improvement.

Although these same techniques can be applied to electromagnetic field measurements at higher frequencies (100 Hz to MHz) much less is known about the scale and temporal variation of noise and signal sources at these frequencies. Furthermore, as discussed below, basis physics likely precludes simple generation of high-frequency electromagnetic signals at seismogenic depths (5–10 km) on active faults in the Earth's crust where the electrical conductivity is more than 0.1 S m^{-1}.

6. Recent Results

Although both electric and magnetic fields are expected to accompany dynamic physical processes in the Earth's crust, simultaneous measurements of both fields are not routinely made. I will therefore discuss separately, electric fields, magnetic fields, and electromagnetic fields during and preceding earthquakes. Magnetic and electric fields generated by earthquakes are termed "seismomagnetic (SM)" and "seismoelectric (SE)" effects. Those preceding earthquakes, or occurring at other times, are termed "tectonomagnetic (TM)" and "tectonoelectric (TE)" effects.

If reliable magnetic and electric field observations (i.e., those unaffected by seismic shaking) are indeed source related, clear offsets should occur at the time of large local earthquakes because the primary energy release occurs at this time. These offsets should scale with the earthquake moment (size) and source geometry. In fact, co-event observations provide a determination of stress sensitivity since the stress redistribution and the source geometry of earthquakes are well-determined (Aki and Richards, 1980). With this calibration, tectonomagnetic and tectonoelectric effects can be quantified and spurious effects identified. Observations without consistent and physically sensible coseismic effects are generally considered suspect.

The following examples are restricted to the strongest data: data recorded independently on more than one instrument, data that are independently supported by other stable geophysical measurement systems, and data for which noise levels have been quantified. Reported measurements made with single instruments or time histories of measurements showing data only for a short period before earthquakes with some "precursive" feature but no coseismic signals, are generally suspect and are not included.

6.1 Seismomagnetic Effects

The primary features of seismomagnetic effects have become clear over the past twenty years with many continuous high-resolution magnetic field measurements in the epicentral regions of moderate-to-large earthquakes. Figure 3 shows a summary of observed SM effects as a function of earthquake moment normalized by epicentral distance. The following features are immediately apparent on this plot:

1. SM effects are observed above the measurement resolution in the near field of earthquakes only when the earthquake magnitude is $M = 6$ or greater.

Au. Q: Can the area below horizontal line be shaded. Please chk.

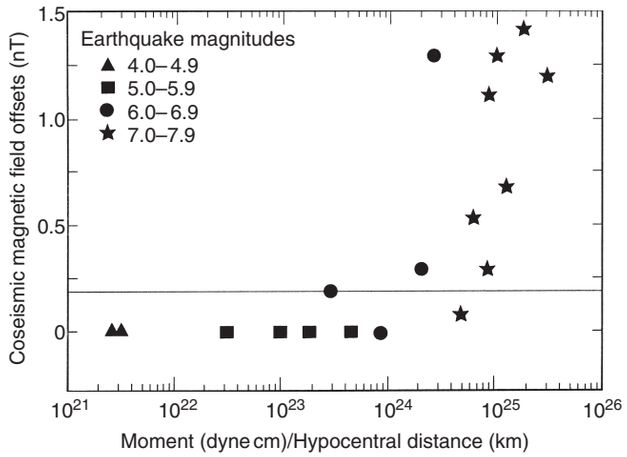

FIGURE 3 Coseismic magnetic field offsets as a function of seismic moment scaled by hypocentral distance. The shaded region below the horizontal line shows the 2-sigma measurement resolution (from Mueller and Johnston, 1998).

2. The amplitudes of SM effects within one rupture length of these earthquakes are not more than 1 nT or so.

Coseismic strain measurements at these same locations for some of these earthquakes are a few microstrain (Johnston *et al*., 1987). Thus, a good rule of thumb for estimating the expected SM effects, where strain observations are available, is to use a scaling factor of 1 nT per microstrain. A similar scaling factor was obtained from correlation between geodetic strain and local geomagnetic fields during aseismic deformation, uplift, and gravity changes in Southern California in the 1980s (Johnston, 1986).

6.1.1 *M* = 7.3 Landers Earthquake (28 June 1992)

An important set of observations of SM effects were made during the 28 July 1992 Landers earthquake (Johnston *et al*., 1994). This earthquake had a moment of 1.1×10^{27} dyne cm and a magnitude of 7.3. Two total field proton magnetometers were in operation at distances of 17.1 and 24.2 km from the earthquake and have recorded synchronously sampled local magnetic fields every 10 min since early 1979 using satellite digital telemetry (Mueller *et al*., 1981). The locations are shown in Figure 4.

The local magnetic field at the magnetometer closest to the earthquake decreased by 1.2 nT while that at the second decreased by 0.7 nT. These values are consistent with a simple SM model of the earthquake in which the fault geometry and slip used are derived from geodetic and seismic inversions of the earthquake data (Johnston *et al*., 1994). Figure 5a shows the differences between data obtained at the two sites OCHM and LSBM for the period 1 day before and after the earthquake. Note that there is no indication of diffusion-like character in the magnetic field offsets that might indicate these effects were generated by fluid flow, nor are there any indications of enhanced low-frequency magnetic noise preceding the earthquake or indications of changing magnetic fields outside the noise in the hours to days before the earthquake. Figure 5b shows the longer-term data for the previous 7 y. The SM effect from the 1986 *M* 6 North Palm Springs earthquake which occurred beneath these same two instruments is clearly evident (Johnston and Mueller, 1987). Similar coseismic results were found for the 1989 *M* 7.1 Loma Prieta earthquake (Mueller and Johnston, 1990).

6.2 Seismoelectric Effects

Seismoelectric observations that show expected scaling with both earthquake moment release and inverse distance cubed are difficult to make because of the sensitivity of electrode contact potential to earthquake shaking. Earlier work by Yamazaki (1974) showed clear correspondence between local coseismic strain steps and coseismic resistivity steps obtained using a Wenner array with a measurement precision of 0.01%. Strain measurements obtained with deep borehole strainmeters (Johnston *et al*., 1987) or with geodetic techniques (e.g., Lisowski *et al*., 1990) do reflect the strain/stress expected from seismically determined models of earthquakes. SE effects should be expected to do likewise. Unfortunately, the effects of shaking on contact potential and on self-potential, as a result of changes in fluid content and fluid chemistry, make these data unreliable reflectors of earthquake stress changes (Ozima *et al*., 1989). Clearly, colocated strain measurements (at tidal sensitivity) and electric field measurements are needed to demonstrate the sensitivity of the electric field measurements to changes in stress/strain in the Earth's crust. This, and observations on multiple sensors with stable electrodes (Petiau and Dupis, 1980; Perrier *et al*., 1997) are necessary to have real confidence in SE measurements as earthquake monitors and perhaps as precursor detectors.

Measurements of electrical resistivity to better than 1% have been made since 1988 in a well-designed experiment installed near Parkfield, California (Park, 1997). Although the expected $M = 6$ earthquake in this region has not occurred, several earthquakes with $M = 5$ have occurred since 1990. None of these earthquakes generated any observable changes in resistivity above the measurement resolution. Observations for three of these dipoles during the times of these earthquakes, and other larger but more distant earthquakes, are shown in Figure 6.

Indirect observations of possible SE signals might be obtained using the magnetotelluric (MT) technique to monitor apparent resistivity in seismically active regions. Even with the best-designed systems using remote referencing systems to reduce noise and obtain stable impedance tensors (Gamble *et al*., 1979), it is difficult to reduce errors below 5% for good soundings and 10–40% for poor soundings (Ernst *et al*., 1993).

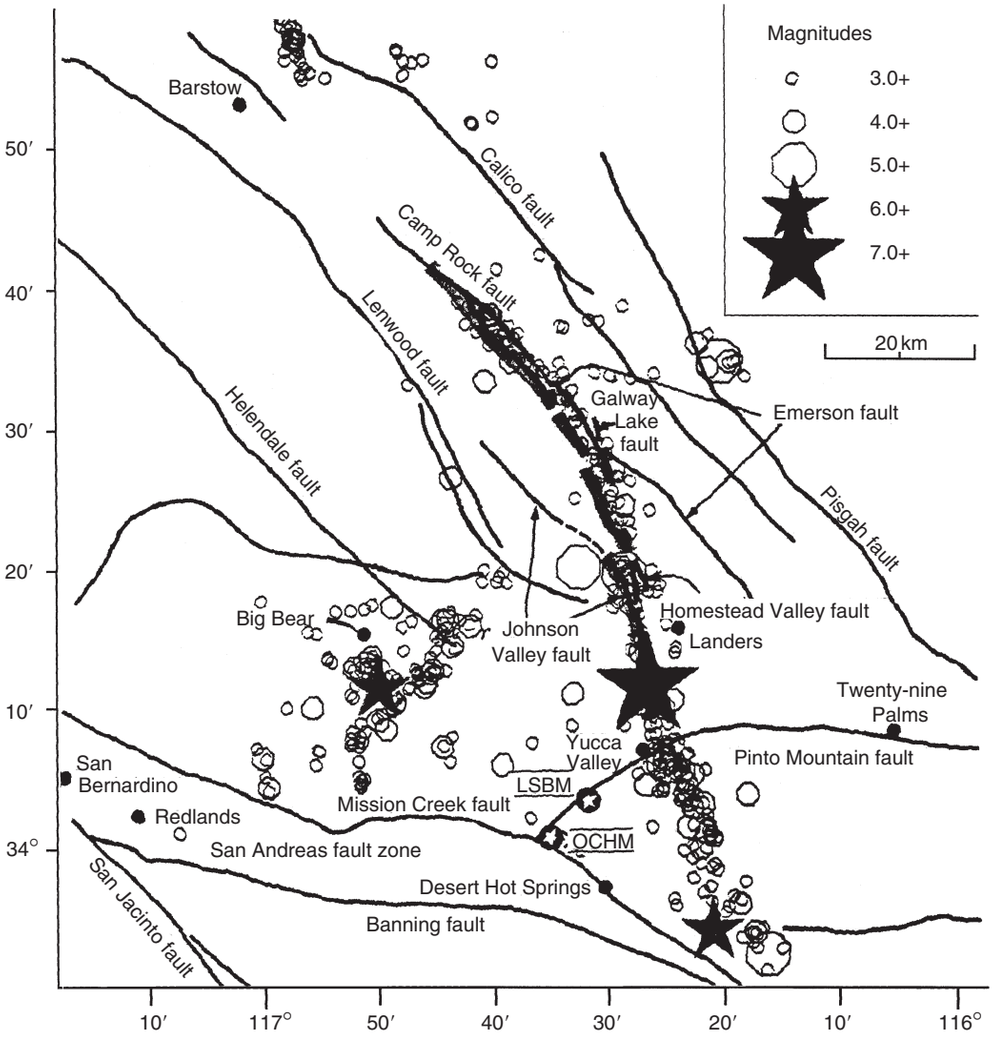

FIGURE 4 Locations of magnetometers, designated LSBM and OCHM (stars inside circles) relative to the epicenter (largest star) of the 28 June 1992 $M = 7.3$ Landers earthquake (from Johnston *et al*., 1994).

Resistivity changes associated with earthquakes are expected (and are observed) to be only a few percent at best. Thus, it is unlikely that this technique will be used generally for detection of resistivity changes. The pioneering work of Honkura *et al*. (1976) still largely defines the limits of observability for MT observations, though some interesting ways of using MT to detect EM emissions with earthquakes have been explored by Rozluski and Yukutake (1993).

6.3 Tectonomagnetic and Possible Precursory Effects

Few indications of convincing longer-term tectonomagnetic events (i.e., durations greater than minutes to weeks) are apparent in multiple near-field magnetometer records obtained along active faults as a result of strain redistribution prior to moderate/large earthquakes. Only one such observation was made in 20 years of data along the San Andreas fault (Mueller and Johnston, 1998). A typical record of long-term magnetic field near active faults is shown in Figure 5b. Signals of more than a few nanoteslas are rare and are of great interest when they occur. If signal amplitudes near active faults are only about a nanotesla, it is unlikely that any reported precursive signals at great epicentral distances are truly earthquake related. Long-term relatively uniform changes, apparently related to crustal loading have been previously reported (Johnston, 1989; Oshiman *et al*., 1983).

The situation may be different at higher frequencies (i.e., ≥ 0.01 Hz). Recent efforts have been concentrated at these higher ultralow frequency (ULF) frequencies as a result, primarily, of fortuitous observation of elevated ULF noise power near the epicenter of the $M = 7.1$ Loma Prieta earthquake of

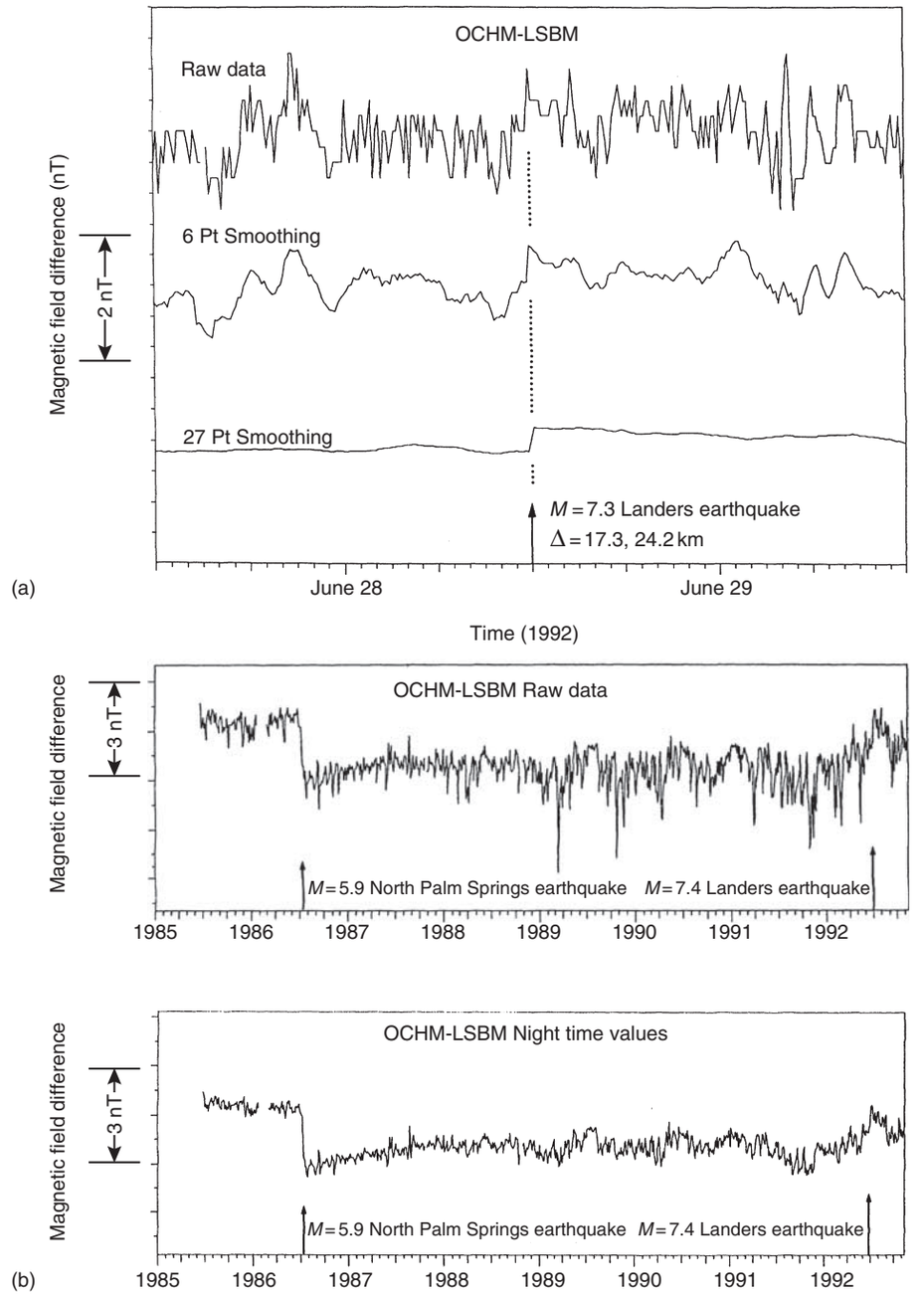

FIGURE 5 (a) Magnetic field differences between OCHM and LSBM (for location see Fig. 4) on the day before and after the Landers earthquake. (b) Similar magnetic field differences from 1985 through 1992 showing the occurrence times of the July 1986 $M = 6$ North Palm Springs earthquake and the June 1992 Landers earthquake (from Johnston *et al*., 1994).

18 October 1989 (Fraser-Smith *et al*., 1990). The magnetometer was located only 7 km from the epicenter (Fig. 7) and recorded increased ULF noise reaching 1.5 nT in amplitude during the two weeks before, and a few hours before the earthquake (Fig. 8). A second system recording ULF/VLF (very low frequency) data 52 km from the earthquake showed no corresponding changes. Similar records were not obtained during the $M = 6.7$ Northridge earthquake at a distance of 81 km from the epicenter (Fraser-Smith *et al*., 1994), for the $M = 7.3$ Landers earthquake, or on magnetic and electric field instruments at the epicenter of the 17 August 1999 $M = 7.4$ Izhmet earthquake in Turkey (Honkura *et al*., 2000).

Table 1 Significant Parkfield and California Earthquakes

Event	Date	Latitude (°N)	Longitude (°N)	M_b	Depth (km)	Distance (km)
A	Oct. 20, 1992	35.93	120.47	4.5	10.0	6.1
B	Apr. 4, 1993	35.94	120.49	4.3	7.6	8.5
C	Nov. 14, 1993	35.95	120.50	4.0	11.6	9.5
D	Dec. 20, 1994	35.92	120.47	5.0	8.6	4.7
E	Oct. 18, 1989	37.04	121.88	7.0	----	180.0
F	Jun. 28, 1992	34.20	116.43	7.2	----	410.0
G	Jan. 17, 1994	34.19	118.57	6.6	----	250.0
H	May 25, 1989	35.87	120.41	3.6	9.6	3.3

E, Loma Prieta; F, Landers; G Northridge. Distance is measured from array center.

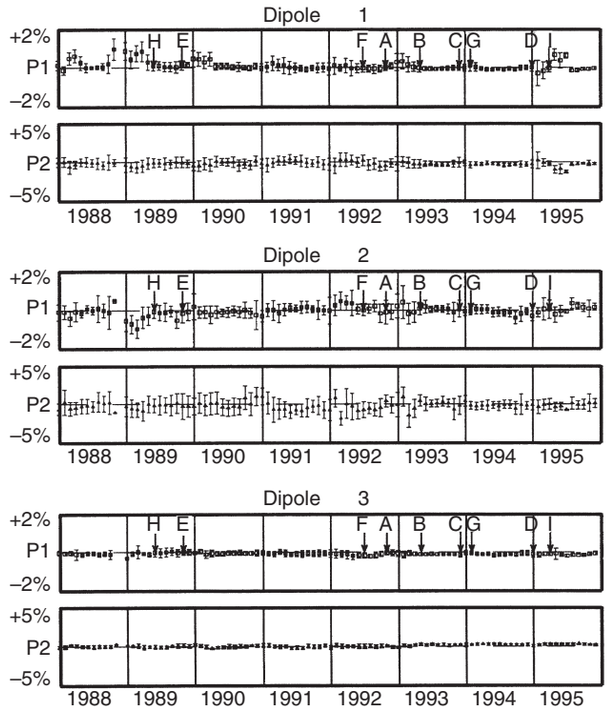

FIGURE 6 Plots of telluric fields at Parkfield, Ca., from 1988 to 1996. Earthquakes A–H (listed in the Table) have occurrence times shown with arrows (from Park, 1997).

Although the Loma Prieta record was recorded on only one magnetometer and therefore violates the multiple instrument requirement discussed above, the instrument was surrounded by independent seismic and strain instrumentation and the data were uncontaminated by cultural noise. For these reasons this example is included here.

For the Loma Prieta observations, Fenoglio *et al*. (1993) have shown that there is no correlation between the ULF anomalies and either the magnitudes or the rates of aftershocks. The absence of signals for these smaller magnitude earthquakes, or for larger earthquakes at greater distances, indicates a localized source for these oscillatory signals. Draganov *et al*. (1991) have suggested a magnetohydrodynamic origin, whereas Fenoglio *et al*. (1995) have suggested an electrokinetic source generated by fluid flow following rupture of high-pressure fluid-filled inclusions in the fault zone.

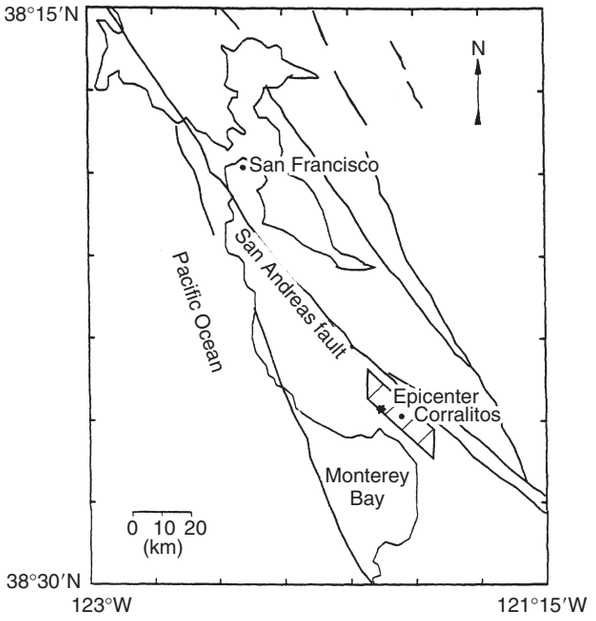

FIGURE 7 Location of ULF receiver at Corralitos, 7 km from the epicenter of the 18 Oct. 1989 $M = 7.1$ Loma Prieta earthquake. A second receiver was located at Stanford University (from Fraser-Smith *et al*., 1990).

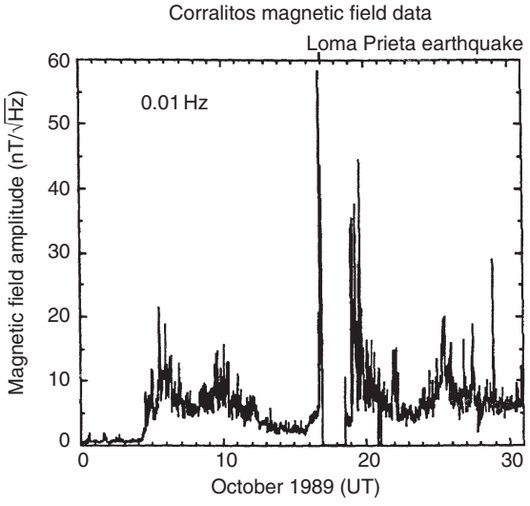

FIGURE 8 Magnetic field amplitude as a function of time during the 17 days before and 14 days after the Loma Prieta earthquake at 00:04 on 17 Oct. 1989 (from Fraser-Smith *et al*., 1990).

6.4 Tectonoelectric and Possible Precursory Effects

The clearest tectonoelectric changes resulting from changes in crustal resistivity were reported in the Tangshan region of China prior to the 1976 Haicheng earthquake (Qian, 1981).

Other interesting, though unexplained changes occurred in the Palmdale region of the San Andreas fault (Madden *et al*., 1993) following the infamous "Palmdale Bulge". These changes occurred in the same region where correlated tectonomagnetic, gravity, strain, and elevations had been reported earlier (Johnston, 1986).

Increased, though controversial, interest in tectonoelectric (TE) phenomena related to earthquakes has occurred during the past ten years, primarily as a result of suggestions in Greece and Japan that short-term geoelectric field transients (SES) of particular form and character precede earthquakes with magnitudes greater than 5 at distances up to several hundreds of kilometers (Varotsos *et al*., 1993a,b; Nagao *et al*., 1996). These transients are recorded on multiple dipoles with different lengths (10–200 m for short arrays and 1–3 km for longer ones) with signal amplitudes of $20\,\text{mv km}^{-1}$ and durations of several minutes. The observation of consistent electric field amplitudes independent of dipole length indicates a local spatially uniform source field. However, there are no corresponding magnetic field transients and no apparent coseismic effects. The SES have been empirically associated with subsequent distant earthquakes in "sensitive" areas (Varotsos *et al*., 1991, 1993a,b, 1996). An example of an SES recorded on multiple orthogonal dipoles together with parallel recordings of magnetic field rate at Ioannina in northwest Greece on 18 April 1995, is shown in Figure 9. This SES was suggested to have preceded a $M = 6.6$ earthquake on 13 May 1995, some 83 km to the northeast. Two other large earthquakes, the $M = 6.6$ on 4 May at Chalkidiki and the 15 June $M = 6.5$ Eratini earthquake, were also suggested to have been predicted by SES on distant stations several weeks before. Similar experiments have been run in Japan, France, and Italy with various levels of claimed success. Nagao *et al*. (1996) suggest that anomalous SES may have been recorded prior to the $M = 7.8$ Hokkaido earthquake in June 1993.

Careful study of the SES recordings indicates that the SES signals do appear to have been generated in the Earth's crust at the observation sites (Uyeshima *et al*., 1998). However, the SES signals have the form expected from rectification/saturation effects of local radio transmissions from high-power transmitters on nearby military bases (Pham *et al*., 1998). Also, no clear physical explanation exists describing how the

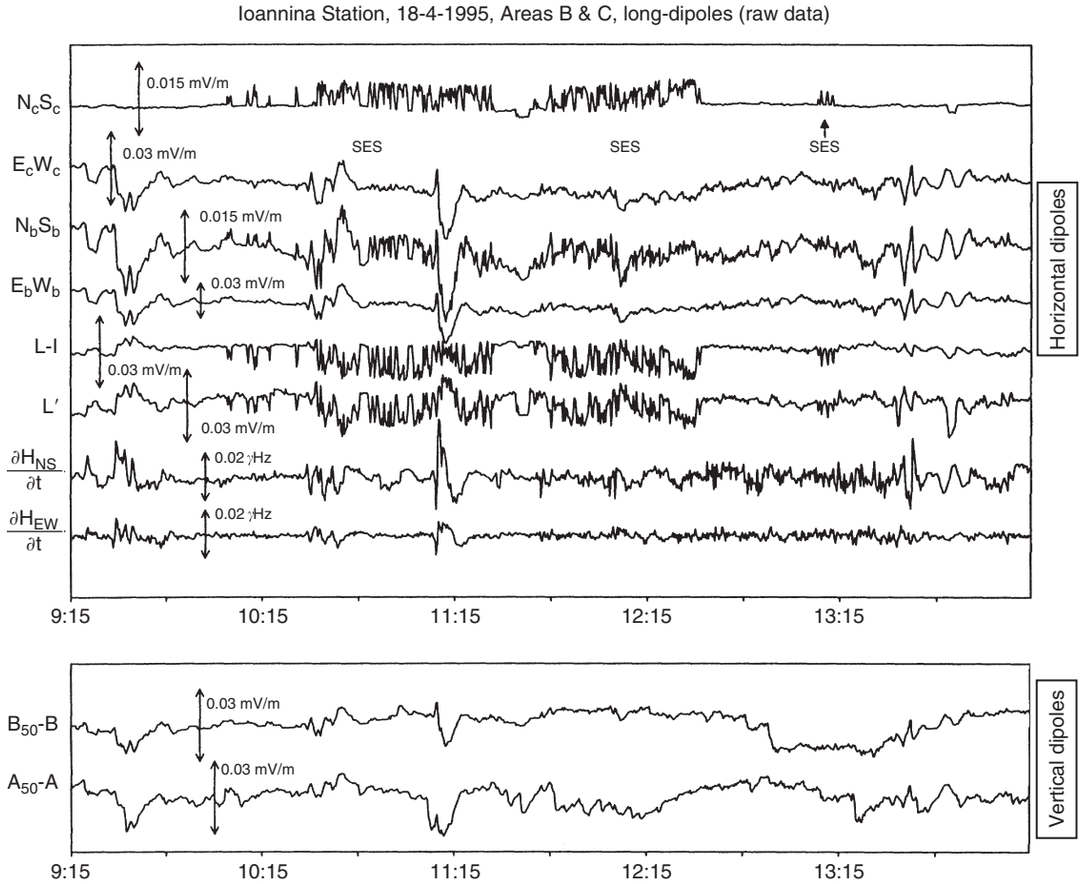

FIGURE 9 Observed SES recorded on multiple dipoles on 19 April 1995 at the Ioannina Station. Simultaneous measurements of magnetic field gradient are shown in the lower two plots (from Varotsos *et al*., 1996).

SES signals can relate to earthquakes occurring sometimes hundreds of kilometers away (Bernard, 1992) whereas sites closer to the earthquake do not record SESs and do not have coseismic effects corresponding to the primary earthquake energy release. Without a clear causal relation, demonstration of statistical significance is controversial (Mulargia and Gasperini, 1992; Hamada, 1993; Shnirman *et al*., 1993; Aceves *et al*., 1996; Varotsos *et al*., 1996; Debate on VAN, 1996; Lighthill, 1996). Better physical understanding is certainly needed. This could be obtained by careful monitoring of the nearby radio transmissions and study of the response of these transmissions on the measuring systems and on the electrical conductivity structure around sites where SESs are recorded. Independent information on the other local sources can be obtained from measurements of high-precision crustal strain, fluid levels in wells, and local pore pressure. The absence of correlative signals in these parameters would further support Pham *et al*.'s (1998) suggestions that these SESs are spuriously generated by local radio transmissions.

6.5 Electromagnetic Effects

Another enigma concerns the generation of high frequency (≥ 1 kHz) electromagnetic emissions prior to moderate earthquakes. Such emissions are reported to have been detected at great distances from these earthquakes (Gokhberg *et al*., 1982; Oike and Ogawa, 1986; Yoshino *et al*., 1985; Yoshino, 1991; Parrot *et al*., 1993; Fujinawa and Takahashi, 1994; Hayakawa and Fujinawa, 1994; Shalimov and Gokhberg, 1998; Kawate *et al*., 1998; Ondoh, 1998) and are also reported to have been detected in satellite data (Molchanov *et al*., 1993; Parrot, 1994), although the statistical significance of these observations is under dispute (Henderson *et al*., 1993; Molchanov *et al*., 1993; Parrot, 1994). This area of research has received attention following reports of changes in the level of 81-kHz electromagnetic radiation around the time of a $M = 6.1$ earthquake at a depth of 81 km beneath the receiver (Gokhberg *et al*., 1982). Radio emissions at 18 MHz were recorded at widely separated receivers in the northern hemisphere for about 15 min before the 16 May 1960 great Chilean $M_w = 9.5$ earthquake (Warwick *et al*., 1982).

Although generation of high frequency electromagnetic radiation can be easily demonstrated in controlled laboratory experiments involving rock fracture in dry rocks (Warwick *et al*., 1982; Brady and Rowell, 1986; Brady, 1992), the physical mechanisms for the generation and the method of propagation of very high frequency (VHF) electromagnetic waves through many tens to hundreds of kilometers of conducting crust (and through the ocean) are not at all clear. Furthermore, the absence of significant local crustal deformation in the epicentral regions of earthquakes during the months to minutes before rupture would seem to strongly constrain the scale of precursive failure. These strain data show that precursive moment release is less than 1% of that occurring coseismically (Johnston *et al*., 1987). As discussed above, simple "skin depth" attenuation arguments preclude sources generating fields, in the kilohertz to megahertz range tens to hundreds of kilometers deep in a conducting crust (1–0.001 S m^{-1}), that would be detectable at the Earth's surface. Appeal to secondary sources at the Earth's surface (Yoshino and Sato, 1993) may avoid this difficulty but the implied large surface strain and displacement fields are not observed.

High frequency disturbances are, of course, generated in the ionosphere as a result of coupled infrasonic waves generated by earthquakes and are readily detected with routine ionospheric monitoring techniques and Global Position System (GPS) measurements (Calais and Minster, 1998). Essentially, the displacement of the Earth's surface by an earthquake acts like a huge piston, generating propagating waves in the atmosphere/ionosphere waveguide (Davies and Archambeau, 1998; see review of gravity waves in the atmosphere by Francis, 1975). Thus, traveling waves in the ionosphere (traveling ionospheric disturbances or TIDs) are a consequence of earthquakes (and volcanic eruptions). EM data at VHF frequencies recorded on ground receivers or by satellite require correction for TID disturbances (and disturbances from other sources) before these data can be identified as direct electromagnetic precursors to earthquakes, or consequences of earthquakes.

7. Conclusions

In summary, improved measurements of magnetic, electric, and electromagnetic fields being made in the epicentral regions of earthquakes around the world, have led to the recognition that observed field perturbations are generated by a variety of EM source processes. It is also clear there are many problems that still need to be resolved. In particular, a clearer understanding of physical processes involved will result from systematic work on:

1. Inclusion of constraints on the various physical mechanisms and models of various processes that are imposed by data from other disciplines such as seismology, geodesy, etc.
2. Demonstration of self-consistency in observations;
3. Determination and inclusion of realistic signal-to-noise estimates.
4. Identification of local noise sources.
5. Checking the implications of these data in other geophysical data obtained in the area. Unusual records can no longer be claimed as precursors just because they precede, or correspond approximately in time, to some local or distant earthquakes. They must be consistent with high-precision seismic and deformation data simultaneously obtained in the near field of each of the earthquakes.

6. Use of reference stations to quantify and remove common-mode noise generated in the ionosphere/magnetosphere.
7. Isolation of the most likely location of signal sources in the Earth's crust consistent with all available data. This appears to be particularly neglected in recent associations of ULF/VLF data with earthquakes.

On the positive side, better understanding has been obtained from well-designed experiments with multiple independent instrument types recording in the same frequency band. This has allowed quantification of at least some of the mechanisms generating electromagnetic fields with tectonic and volcanic activity. It now seems likely that:

1. Stress-generated magnetic effects (piezomagnetic effects) are readily observed as a result of crustal stress drops for earthquakes with $M \geq 6$ such as during the $M = 7.1$ Loma Prieta earthquake on the San Andreas fault in 1989, the $M = 7.3$ Landers earthquake in 1992 and the $M = 6$ North Palm Springs earthquake in 1986.
2. Precursive EM fields are rare in both low frequency and high frequency electromagnetic field data above the measurement resolution of 0.01 nT at 100 Hz to a few nT at hours to days for local magnetic fields and $0.01\,\mathrm{mv\,km^{-1}}$ at 100 Hz to $1\,\mathrm{mv\,km^{-1}}$ at hours to days for electric fields.
3. Electrokinetic effects probably occurred during the $M = 7.1$ Loma Prieta earthquake in 1989.

Finally, it is obvious that more complete observational arrays are needed in critical locations to provide a sound database for EM studies. Earthquakes occur infrequently and great skill is needed to "catch" these events with adequate arrays so we can better understand the physical processes involved.

Acknowledgments

I would like to thank Steve Park, Tony Fraser-Smith, Bob Mueller and other colleagues for stimulating discussions. Larry Byer and Yoshimori Honkura provided useful reviews.

References

Aceves, R.L., *et al*. (1996). *Geophys. Res. Lett*. **23**, 1425–1428.
Aki, K. and P.G. Richards (1980). "Quantitative Seismology," Freeman Press.
Ahmad, M. (1964). *Geophys. Prospect*. **12**, 49–64.
Baird, G.A. and P.S. Kennan (1985). *Tectonophysics* **111**, 147–l54.
Banks, P.O., *et al*. (1991). *J. Geophys. Res.* **96**, 21575–21582.
Barsukov, O.M. (1972). *Tectonophysics* **14**, 273–277.
Bernard, P. (1992). *J. Geophys. Res.* **97**, 17531–17546.
Blanchard, D.C. (1964). *Nature* **201**, 1164–1166.
Brace, W.F. (1975). *Pure Appl. Geophys.* **113**, 207–217.
Brace, W.F. (1980). *Int. J. Rock Mech.* **17**, 876–893.
Brace, W.F. and A.S. Orange (1968a). *J. Geophys. Res.* **73**, 1443–1445.
Brace, W.F. and A.S. Orange (1968b). *J. Geophys. Res.* **73**, 5407–5420.
Brace, W.F., *et al*. (1965). *J. Geophys. Res.* **70**, 5669–5678.
Brady, B.T. (1992). In: "Report 92-15, IGPP," University of California, Riverside.
Brady, B.T. and G.A. Rowell (1986). *Nature*. **321**, 488–490.
Calais, E. and J.B. Minster (1998). *Phys. Earth. Planet. Inter*. **105**, 167–181.
Chalmers, A. (1976). "Atmospheric Electricity," Pergamon.
Davies, J.B. and C.B. Archambeau (1998). *Phys. Earth. Planet. Inter*. **105**, 183–199.
Davis, P.M. and M.J.S. Johnston (1983). *J. Geophys. Res.* **88**, 9452–9460.
Davis, P.M., *et al*. (1979). *Phys. Earth Planet. Inter*. **19**, 331–336.
Davis, P.M., *et al*. (1981). *J. Geophys. Res.* **86**, 1731–1737.
Davis, P.M., *et al*. (1984). *Geophys. Res. Lett*. **11**, 225–228.
Debate on VAN (1996). *Geophys. Res. Lett*. **23**, 1291–1452.
Dobrovolsky, I.P., *et al*. (1989). *Phys. Earth Planet. Inter*. **57**, 144–156.
Dologlou-Revelioti, E. and P. Varotsos (1986). *Geophysics*. **59**, 177–182.
Draganov, A.B., *et al*. (1991). *Geophys. Res. Lett*. **18**, 1127–1130.
Dzurisin, D., *et al*. (1990). *Bull. Seismol. Soc. Am.* **95**, 2763–2780.
Emeleus, T.G. (1977). *J. Volc. Geotherm. Res.* **2**, 343–359.
Ernst, T., *et al*. (1993). *Tectonophysics* **224**, 141–148.
Fenoglio, M.A., *et al*. (1993). *Bull. Seismol. Soc. Am.* **83**, 347–357.
Fenoglio, M.A., *et al*. (1995). *J. Geophys. Res.* **100**, 12951–12958.
Finkelstein, D., *et al*. (1973). *J. Geophys. Res.* **78**, 992–993.
Fitterman, D.V. (1978). *J. Geophys. Res.* **83**, 5923–5928.
Fitterman, D.V. (1979). *J. Geophys. Res.* **84**, 6031–6040.
Fitterman, D.V. (1981). *J. Geophys. Res.* **86**, 9585–9588.
Fitterman, D.V. and T.R. Madden (1977). *J. Geophys. Res.* **82**, 5401–5408.
Francis, S.H. (1975). *J. Atmos. Terr. Phys.* **37**, 1011–1054.
Fraser, D.C. (1966). *Geophys. J. R. Astron. Soc*. **11**, 507–517.
Fraser-Smith, A.C., *et al*. (1990). *Geophys. Res. Lett*. **17**, 1465–1468.
Fraser-Smith, A.C., *et al*. (1994). *Geophys. Res. Lett*. **21**, 2195–2198.
Freund, F., *et al*. (1992). In: "Report 92-15, IGPP," University of California, Riverside.
Fujinawa, Y., *et al*. (1992). *Geophys. Res. Lett*. **19**, 9–12.
Fujinawa, Y. and K. Takahashi (1994). In: "Electromagnetic Phenomena Related to Earthquake Prediction," Terra Science Publishers.
Gamble, T.D., *et al*. (1979). *Geophysics* **44**, 53–58.
Gokhberg, M.B., *et al*. (1982). *J. Geophys. Res*. **87**, 7824–7828.
Hamada, K. (1992). *Tectonophysics* **224**, 203–210.
Hamano, Y., *et al*. (1989). *J. Geomagn. Geoelectr*. **41**, 203–220.
Hayakawa, M. and F. Fujinawa (Eds.) (1994). "Electromagnetic Phenomena Related to Earthquake Prediction," Terra Science Publishers.
Henderson, T.R., *et al*. (1993). *J. Geophys. Res.* **98**, 9503–9509.
Honkura, Y. and Y. Kuwata (1993). *Tectonophysics* **224**, 257–264.
Honkura, Y., *et al*. (1976). *Tectonophysics* **34**, 219–230.
Honkura, Y., *et al*. (2000). *Trans. Am. Geophys. Un.* **81**, F891.
Hurst, A.W. and D.A. Christoffel (1973). *NZ J. Geol. Geophys.* **16**, 965–972.

Ishido, T. and M. Mizutani (1981). *J. Geophys. Res.* **86**, 1763–1775.
Johnston, M.J.S. (1978). *J. Geomagn. Geoelectr.* **30**, 511–522.
Johnston, M.J.S. (1986). *J. Geomagn. Geoelectr.* **38**, 933–947.
Johnston, M.J.S. (1989). *Phys. Earth Planet. Inter.* **57**, 47–63.
Johnson, M.J.S. (1997). *Surv. Geophys.* **18**, 441–475.
Johnston, M.J.S. and R.J. Mueller (1987). *Science* **237**, 1201–1203.
Johnston, M.J.S. and M. Parrot (Eds.) (1989). *Phys. Earth Planet. Inter.* **57**, 1–177.
Johnston, M.J.S. and M. Parrot (Eds.) (1998). *Phys. Earth Planet. Inter.* **105**, 109–207.
Johnston, M.J.S., *et al.* (1984). *J. Geomagn. Geoelectr.* **36**, 83–95.
Johnston, M.J.S., *et al.* (1987). *Tectonophysics* **144**, 189–206.
Johnston, M.J.S., *et al.* (1994). *Bull. Seismol. Soc. Am.* **84**, 792–798.
Kalashnikov, A.C. (1954). *Trans. Geofiz. Inst. Akad. Nauk. SSSR, Sb. Statei* **25**, 162–180.
Kalashnikov, A.C. and S.P. Kapitsa (1952). *Proc. Acad. Sci. USSR* **86**, 521–523.
Kapitsa, S.P. (1955). *Izv. Akad. Nauk. SSSR, Ser. Geofiz.* **6**, 489–504.
Kawate, R., *et al.* (1998). *Phys. Earth. Planet. Inter.* **105**, 229–238.
Kean, W.F., *et al.* (1976). *J. Geophys. Res.* **85**, 861–872.
Kern, J.W. (1961). *J. Geophys. Res.* **66**, 3801–3805.
Lighthill, J. (Ed.) (1996). "A Critical Review of VAN," World Science Press.
Lisowski, M., *et al.* (1990). *Geophys. Res. Lett.* **17**, 1437–1440.
Lockner, D.A. and J.D. Byerlee (1985). *Geophys. Res. Lett.* **12**, 211–214.
Lockner, D.A. and J.D. Byerlee (1986). *Pure Appl. Geophys.* **124**, 659–676.
Lockner, D.A., *et al.* (1991). *Nature* **350**, 39–42.
Lowell, F. and A.C. Rose-Innes (1980). *Adv. Phys.* **29**, 947–1023.
Madden, T.R., *et al.* (1993). *J. Geophys. Res.* **98**, 795–808.
Mascart, E. (1887). *Comptes Rendus* **115**, 607–634.
Matteson, M.J. (1971). *J. Colloid. Interface Sci.* **37**, 879–890.
Martin III, R.J. (1980). *J. Geomagn. Geoelectr.* **32**, 741–755.
Milne, J. (1890). *Trans. Seismol. Soc. Jpn.* **15**, 135.
Milne, J. (1894). *Seismol. J. Jpn.* **3**, 23.
Mizutani, H. and T. Ishido (1976). *J. Geomagn. Geoelectr.* **28**, l79–188.
Molchanov, O.A., *et al.* (1993). *Ann. Geophys.* **11**, 431–440.
Mori, T., *et al.* (1993). *Phys. Earth. Planet. Inter.* **77**, 1–12.
Mueller, R.J. and M.J.S. Johnston (1990). *Geophys. Res. Lett.* **17**, 1231–1234.
Mueller, R.J. and M.J.S. Johnston (1998). *Phys. Earth. Planet. Inter.* **105**, 131–144.
Mueller, R.J., *et al.* (1981). *US Geol. Surv. Open-file Report* 81-1346.
Mulargia, F. and P. Gasperini (1992). *Geophys. J. Int.* **111**, 32–44.
Nagao, T., *et al.* (1996). In: "A Critical Review of VAN," pp. 292–300, World Science Press.
Nagata, T. (1969). *Tectonophysics* **21**, 427–445.
Nourbehecht, B. (1963). PhD. thesis, Massachussetts Institute of Technology, Cambridge.
Ohnaka, M. and H. Kinoshita (1968). *J. Geomagn. Geoelectr.* **20**, 93–99.
Oike, K. and T. Ogawa (1986). *J. Geomagn. Geoelectr.* **38**, 1031–1041.
Ondoh, T. (1998). *Phys. Earth Planet. Inter.* **105**, 261–270.
Oshiman, N., *et al.* (1983). *Earthq. Predict. Res.* **2**, 209–219.
Ozima, M., *et al.* (1989). *J. Geomagn. Geoelectr.* **41**, 945–962.
Park, S.K. (1991). *J. Geophys. Res.* **96**, 14211–14237.
Park, S.K. (1996). *Surv. Geophys.* **17**, 493–516.
Park, S.K. (1997). *J. Geophys. Res.* **102**, 24545–24559.
Park, S.K. and D.V. Fitterman (1990). *J. Geophys. Res.* **95**, 15557–15571.
Park, S.K., *et al.* (1993). *Rev. Geophys.* **31**, 117–132.
Parrot, M. (1994). *J. Geophys. Res.* **99**, 23339–23349.
Parrot, M. and M.J.S. Johnston (Eds.) (1993). *Phys. Earth Planet. Inter.* **77**, 1–137.
Parrot, M., *et al.* (1993). *Phys. Earth Planet. Inter.* **77**, 65–83.
Perrier, F.E., *et al.* (1997). *J. Geomagn. Geoelectr.* **49**, 1677–1696.
Petiau, G. and A. Dupis (1980). *Geophys. Prospect.* **28**, 792–804.
Pham, V.N., *et al.* (1998). *Geophys. Res. Lett.* **25**, 2229–2232.
Pike, S.J., *et al.* (1981). *J. Geophys. Res.* **33**, 449–466.
Qian, J. (1981). "Proc. Int. Symposium on Earthquake Prediction," Chinese Seismology Press.
Reid, H.F. (1914). *Terr. Mag.* **19**, 57–189.
Revol, J., *et al.* (1977). *Earth Planet. Sci. Lett.* **37**, 296–306.
Rikitake, T. (1966). *Bull. Earthq. Res. Inst.* **44**, 1041–1070.
Rikitake, T. (1968). *Tectonophysics* **6**, 59–68.
Rikitake, T. (1976). "Earthquake Prediction," Elsevier.
Rikitake, T. and **Yokoyama** (1955). *J. Geophys. Res.* **60**, 165–172.
Rozluski, C.P. and T. Yukutake (1993). *Acta Geophys. Pol.* **41**, 17–26.
Sasai, Y. (1980). *Bull. Earthq. Res. Inst.* **55**, 387–447.
Sasai, Y. (1983). *Bull. Earthq. Res. Inst.* **58**, 763–785.
Sasai, Y. (1991a). *J. Geomagn. Geoelectr.* **43**, 21–64.
Sasai, Y. (1991b). *Bull. Earthq. Res. Inst.* **66**, 585–722.
Sasai, Y. (1994). *J. Geomagn. Geoelectr.* **42**, 329–340.
Sasaoka, H., *et al.* (1998). *Geophys. Res. Lett.* **25**, 2225–2228.
Shalimov, S. and M. Gokhberg (1998). *Phys. Earth. Planet. Inter.* **105**, 211–218.
Shamsi, S. and F.D. Stacey (1969). *Bull. Seismol. Soc. Am.* **59**, 1435–1448.
Shercliff, J.A. (1965). "A Textbook of Magnetohydrodynamics," Pergamon Press.
Shnirman, M., *et al.* (1993). *Tectonophysics* **224**, 211–221.
Stacey, F.D. (1962). *Philos. Mag.* **7**, 551–556.
Stacey, F.D. (1964). *Pure Appl. Geophys.* **58**, 5–22.
Stacey, F.D. (1992). "Physics of the Earth," 3rd edn. Brookfield Press.
Stacey, F.D. and S.K. Banerjee (1974). "The Physical Principles of Rock Magnetism," Elsevier.
Stacey, F.D. and M.J.S. Johnston (1972). *Pure Appl. Geophys.* **97**, 146–155.
Stacey, F.D., *et al.* (1965). *Pure Appl. Geophys.* **62**, 96–104.
Tanaka, Y. (1993). *J. Volc. Geotherm. Res.* **56**, 319–338.
Tanaka, T. (1995). *J. Geomagn. Geoelectr.* **47**, 325–336.
Tuck, G.T., *et al.* (1977). *Tectonophysics* **39**, 7–11.
Utada, H. (1993). *Tectonophysics* **224**, 149–152.
Utada, H., *et al.* (2000). *Earth, Planets Space* **52**, 91–103.
Uyeshima, M., *et al.* (1998). *Phys. Earth. Planet Inter.* **105**, 153–166.
Varotsos, P. and K. Alexopoulos (1987). *Tectonophysics* **136**, 335–339.
Varotsos, P. and M. Lazaridou (1991). *Tectonophysics* **188**, 321–347.
Varotsos, P., *et al.* (1993a). *Tectonophysics* **224**, 1–38.
Varotsos, P., *et al.* (1993b). *Tectonophysics* **224**, 269–288.
Varotsos, P., *et al.* (1996). *Acta. Geophys. Pol.* **44**, 301–327.
Ware, R.H., *et al.* (1985). *J. Geomagn. Geoelectr.* **37**, 1051–1061.

Au. Q: Please provide initials.

Warwick, J.W., *et al*. (1982). *J. Geophys. Res.* **87**, 2851–2859.
Williamson, S.J. and L. Kaufman (1981). *J. Magn. Mater.* **22**, 129–201.
Wilson, E. (1922). *Proc. R. Soc. A.* **101**, 445–452.
Yamazaki, Y. (1965). *Bull. Earthq. Res. Inst.* **44**, 783–802.
Yamazaki, Y. (1974). *Tectonophysics* **22**, 159–171.
Yoshino, T., *et al*. (1985). *Ann. Geophys.* **3**, 727–730.
Yoshino, T. (1991). *J. Sci. Explor.* **5**, 121–144.
Yoshino, T. and H. Sato (1993). *JISHIN* **16**, 8–24.
Zlotnicki, J. and J.L. Le Mouel (1988). *J. Geophys. Res.* **93**, 9157–9171.
Zlotnicki, J. and J.L. Le Mouel (1990). *Nature* **343**, 633–636.

Editor's Note

Due to space limitations, references with full citation are given in the file "Johnston2FullReferences.tex" on the Handbook CD-ROM, under the directory \38Johnston2. An equivalent PDF file is also provided on the CD. Please see also Chapter 32, Rock failure and earthquake, by Lockner and Beeler; and Chapter 72, Earthquake prediction: an overview, by Kanamori.